Supplementary Information (SI) for Journal of Materials Chemistry A.
This journal is © The Royal Society of Chemistry 2025

Supplementary Information

Rapid Synthesis of Highly Dispersed FeCoNiRuPt High-Entropy Alloy Bifunctional Electrocatalyst and Exploration of the Catalytic Mechanism

Yong Wei [‡a], Zhihao Hu [‡a], Ke Wang [a], Dongxu Wu [a], Feng Cheng [*a], Ningyan Cheng [*a], Chuanqiang Wu [*a], Binghui Ge [a], and Li Song [*b]

a. Information Materials and Intelligent Sensing Laboratory of Anhui Province Institutes of Physical Science and Information Technology, Anhui University, Hefei, Anhui, 230601. China.

b. National Synchrotron Radiation Lab, University of Science and Technology of China, Hefei, Anhui 230029, China.

*Corresponding authers:
E-mail address: wucq@ahu.edu.cn (C. Q. Wu);
chengfeng769@126.com (F. Cheng);
ningyancheng@ahu.edu.cn (N. Y. Cheng);
song2012@ustc.edu.cn (L. Song)

‡ Both authors contributed equally to the manuscript.

Experimental Section

Chemicals and Materials

Ferric(III) chloride ($FeCl_3$, 99.9%), cobalt(II) chloride hexahydrate ($CoCl_2·6H_2O$, 98%), nickel(III) chloride hexahydrate ($NiCl_3·6H_2O$, 98%), and potassium chloroplatinate (K_2PtCl_6, 98%) were purchased from Shanghai Aladdin Biochemical Technology Co. Ltd. Ruthenium(III) chloride ($RuCl_3$, 99%) were purchased from Energy Chemical. Graphene oxide dispersion (GO, 5 mg/mL) were purchased from XFNANO. All chemicals used were of analytical grade and were utilized without further purification. Deionized water (18.25 MΩ) was employed for all experiments.

Synthsis of $Fe_2Co_2Ni_2Ru_2Pt_{0.5}$

Prepare 0.01 mol/L of the above metal salt solutions. Take 2 mL $FeCl_3$ solution (2 mmol), 2 mL $CoCl_2$ solution (2 mmol), 2 mL $NiCl_2$ solution (2 mmol), 2 mL $RuCl_3$ solution (2 mmol), 0.5 mL K_2PtCl_6 solution (0.5 mmol) and 6 mL GO dispersion. Mix them in a 20 mL brown vial and dilute to 20 mL with deionized water. Thus, the FCNRP-0.5 HEA NPs/rGO precursor solution is obtained. Next, sonicate the obtained precursor solution for 30 min, and then electromagnetically stir it for 1 h. After that, freeze the mixed solution with liquid nitrogen and cool it in a vacuum freeze dryer for later use. Subsequently, place the cold-dried samples in a vacuum flask and wash them with a proper solvent under argon atmosphere once. Finally, heat the samples rapidly by microwave until there is no combustion. In this way, $Fe_2Co_2Ni_2Ru_2Pt_{0.5}$ is obtained.

Synthsis of $Fe_2Co_2Ni_2Ru_2Pt_2$

$Fe_2Co_2Ni_2Ru_2Pt_2$ were synthesized in a similar way as $Fe_2Co_2Ni_2Ru_2Pt_{0.5}$. First, the amount of K_2PtCl_6 solution was increased to 2 mL (2 mmol) in the previously mentioned formulation, and the same amount was used for the other solutions. Then, these solutions were mixed in a 20 mL brown vial and diluted to 20 mL with deionized water to obtain the $Fe_2Co_2Ni_2Ru_2Pt_2$ precursor solution. The subsequent sonication,

stirring, cold-drying and MRH of the precursor solution were identical to those in the synthesis of $Fe_2Co_2Ni_2Ru_2Pt_{0.5}$ in terms of operating parameters and reaction conditions.

Synthesis of rGO

Take 6 mL of GO suspension and place it in a 20 mL vial. Then, dilute it to 20 mL with deionized water. After that, the subsequent sonication, stirring, cold-drying and MRH of the precursor solution were identical to those in the synthesis of $Fe_2Co_2Ni_2Ru_2Pt_{0.5}$ in terms of operating parameters and reaction conditions.

Characterizations

The phase information of the HEA was identified by using an X-ray diffractometer (XRD, Rigaku) with a Cu K_α radiation source (λ = 0.154084 nm). The diffraction angle was scanned from 35° to 90° at a rate of 20° per minute. For microstructure observation, a Carl Zeiss Crossbeam 550 FIB-SEM scanning electron microscope, a TEM (JEM-F200), and a AC-TEM (JEM-ARM200F) equipped with an energy-dispersive X-ray spectrometer were employed. The surface of the HEA was analyzed by an XPS instrument with the model of ECSA-LAB250Xi.The elemental composition ratio of the HEA was obtained through the ICP-OES test. The N_2 adsorption/desorption isotherm and pore size distribution curves of the material at 78 K were tested using the Micromeritics Tristar (Micromeritics ASAP 2460) instrument. Moreover, the functional groups of the material were analyzed by means of laser confocal Raman spectroscopy (inVia-Reflex) and FTIR (Vertex80 + Hyperion2000).

Electrochemical Measurement

All electrochemical measurements are performed in a standard three-electrode system using a CHI 760E potentiostat (Shanghai Chenhua). Graphite rods and silver/silver chloride electrodes (Ag/AgCl) calibrated against the reversible hydrogen electrode (RHE) are used as counter and reference electrodes, respectively. The working

electrode is prepared as follows: 2 mg of the catalyst sample is dispersed in a mixture of isopropanol (325 μL), deionized water (125 μL), and 5% Nafion (50 μL). The mixture is then sonicated for 1 h until a homogeneous dispersion is formed. Then, a volume of 5 μL of the catalyst dispersion is dropped onto a GC working electrode (with a loaded mass density of 0.134 mg cm^{-2}) using a pipette and left to dry naturally before electrochemical measurements. The working electrode preparation process for the commercial 20% Pt/C catalyst and IrO_2 catalyst is similar to that of the catalyst samples described above. After the working electrode is prepared, the HER test is performed using a CHI 760E potentiostat with a scan rate of 0.1 V s^{-1} in 1 M KOH solution and 0.5 M H_2SO_4 solution, respectively. The scanning potential (vs RHE) interval in 1 M KOH solution is -0.3 ~ 0 V, and the scanning potential (vs RHE) interval in 0.5 M H_2SO_4 solution is -0.2 ~ 0 V. For the OER test, a linear scanning voltammetry test with a scan rate of 0.1 V s^{-1} is performed in 1 M KOH solution, and the scanning potential (vs RHE) range is 0.2 ~ 0.4 V. Prior to each HER (or OER) linear scanning voltammetry test, a voltammetry cycle is performed at a scan rate of 0.1 V s^{-1} for 20 cycles to activate the catalyst on the GC electrode. EIS tests are performed in the frequency range from 0.01 Hz to 100 KHz with an AC amplitude of 5 mV. The open-circuit potential at sweep velocities of 20 mV s^{-1}, 40 mV s^{-1}, 60 mV s^{-1}, 80 mV s^{-1}, 100 mV s^{-1} and 120 mV s^{-1} is measured using the C_{dl} to calculate the ECSA of the catalyst.

Supplementary Figures

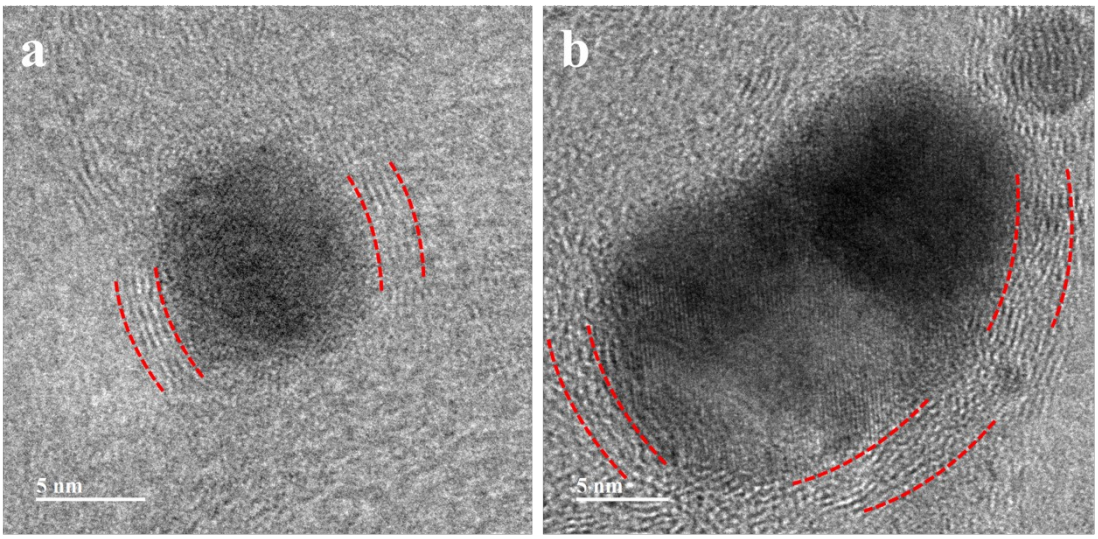

Fig. S1 HRTEM of $Fe_2Co_2Ni_2Ru_2Pt_{0.5}$, where the red dashed line indicates the outer graphene coating layer.

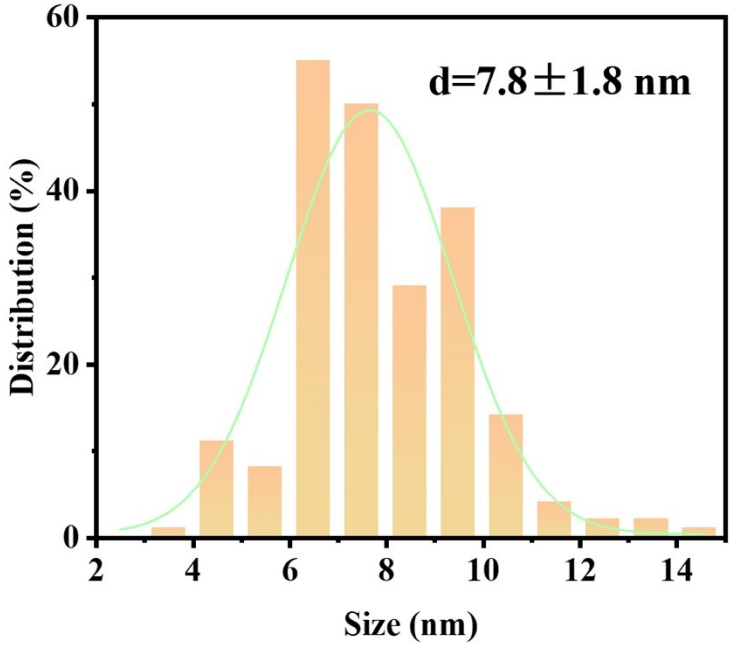

Fig.S2 Particle size statistics of $Fe_2Co_2Ni_2Ru_2Pt_{0.5}$.

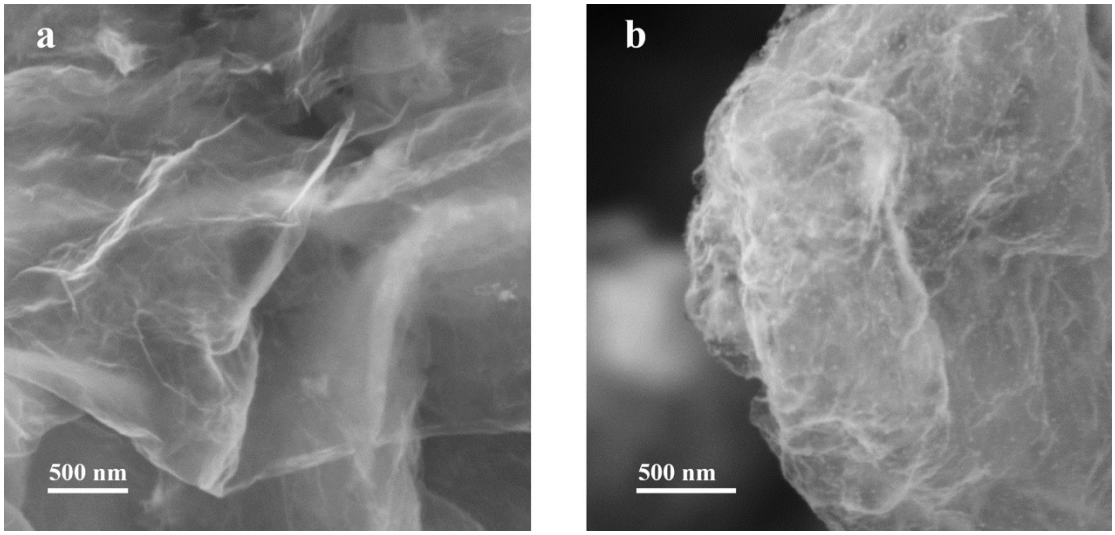

Fig. S3 SEM images of synthesized $Fe_2Co_2Ni_2Ru_2Pt_{0.5}$, (a) low-magnification SEM image, (b) high-magnification SEM image.

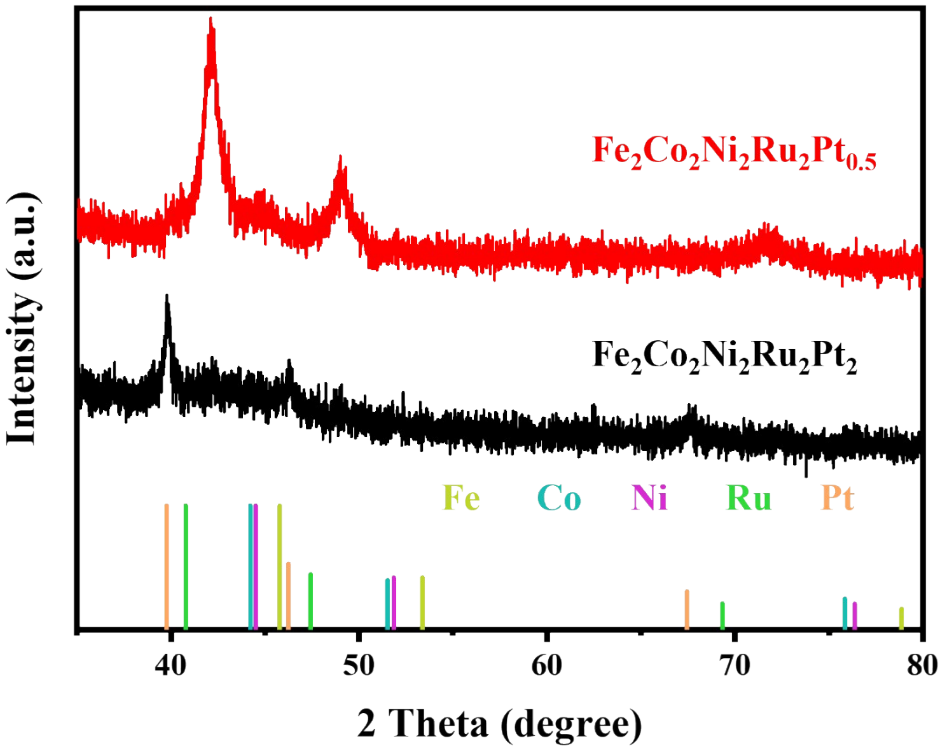

Fig. S4 XRD patterns of two synthetic $Fe_2Co_2Ni_2Ru_2Pt_x$.

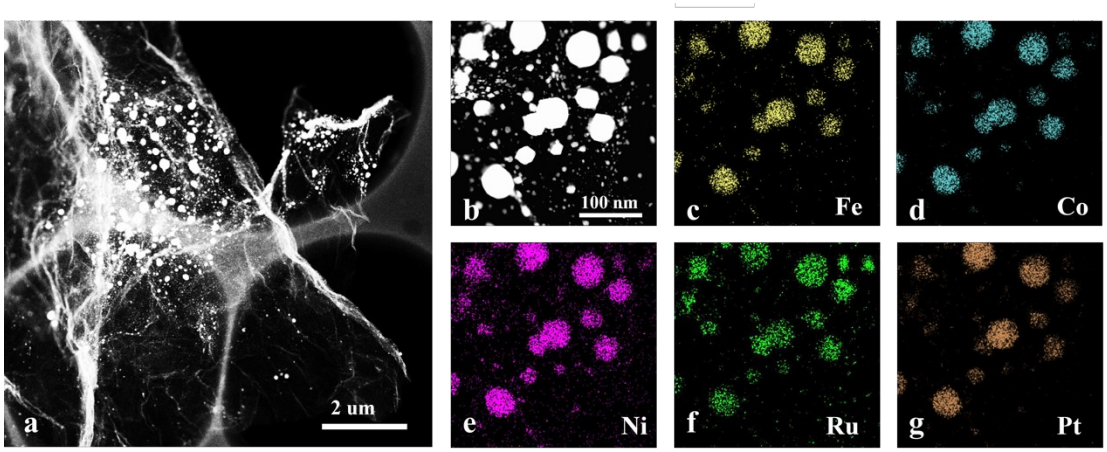

Fig. S5 (a) HAADF-STEM images of $Fe_2Co_2Ni_2Ru_2Pt_2$, (b-g) magnified HAADF-STEM images of multiple particles of $Fe_2Co_2Ni_2Ru_2Pt_2$ and corresponding EDS element mapping images.

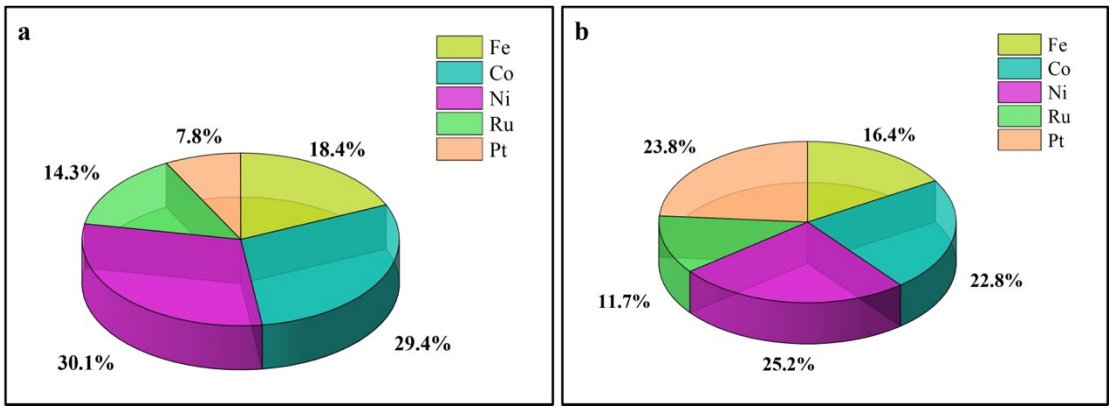

Fig. S6 ICP-OES plots of two synthesized $Fe_2Co_2Ni_2Ru_2Pt_x$. (a) ICP-OES plot of $Fe_2Co_2Ni_2Ru_2Pt_{0.5}$. (b) ICP-OES plot of $Fe_2Co_2Ni_2Ru_2Pt_2$.

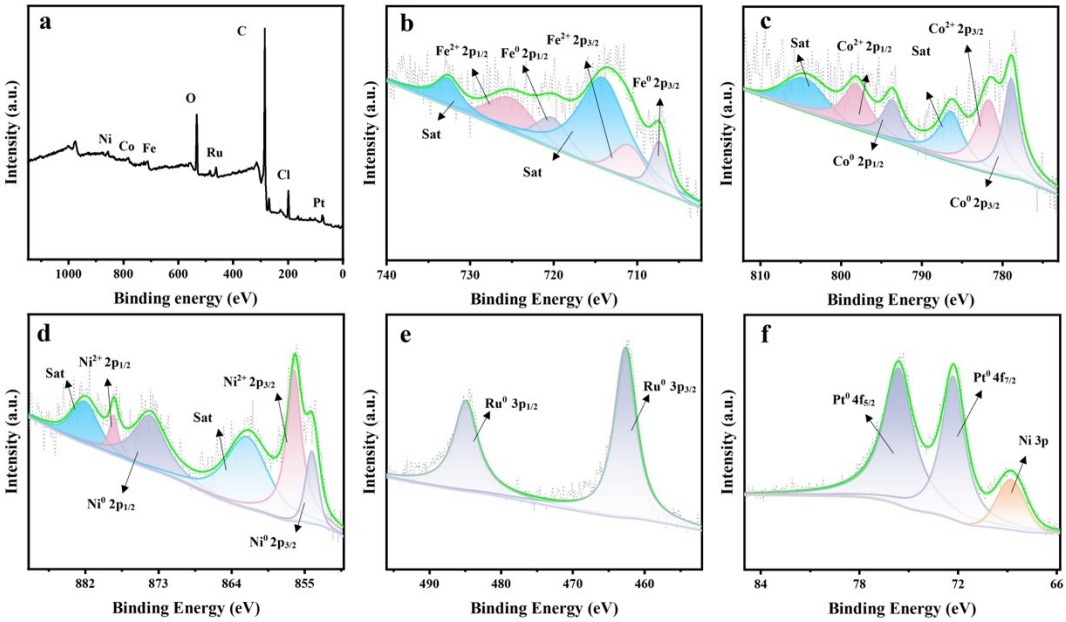

Fig. S7 (a) XPS full spectrum of $Fe_2Co_2Ni_2Ru_2Pt_{0.5}$; (b-f) high-resolution XPS spectra of $Fe_2Co_2Ni_2Ru_2Pt_{0.5}$ for Fe 2p, Co 2p, Ni 2p, Ru 3p, and Pt 4f, respectively.

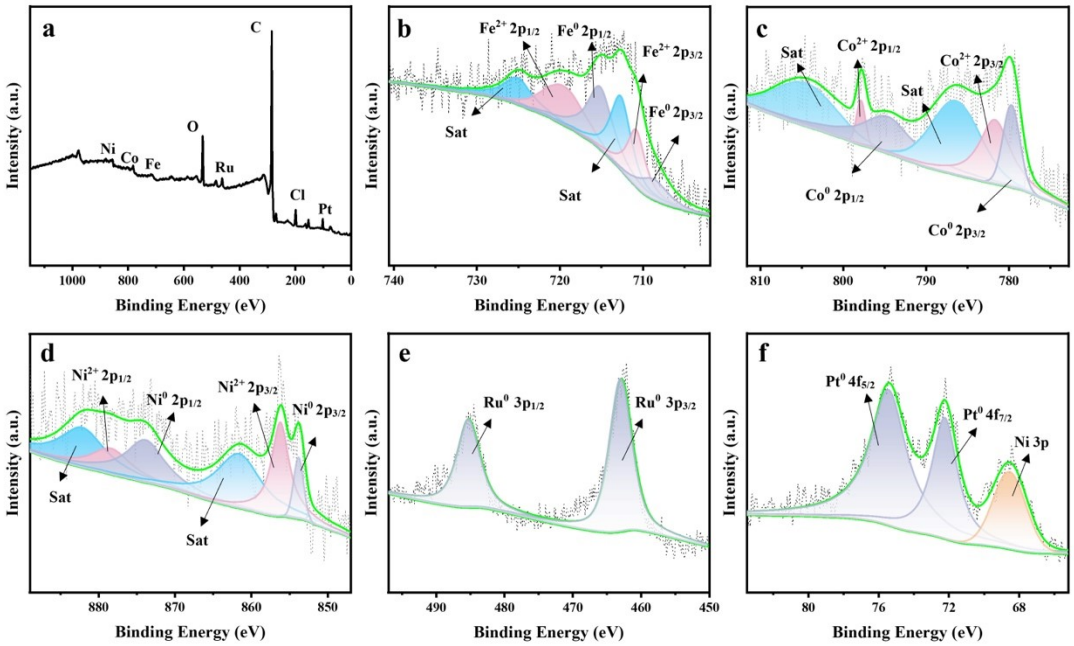

Fig. S8 (a) XPS full spectrum of $Fe_2Co_2Ni_2Ru_2Pt_2$; (b-f) high-resolution XPS spectra of $Fe_2Co_2Ni_2Ru_2Pt_2$ for Fe 2p, Co 2p, Ni 2p, Ru 3p, and Pt 4f, respectively.

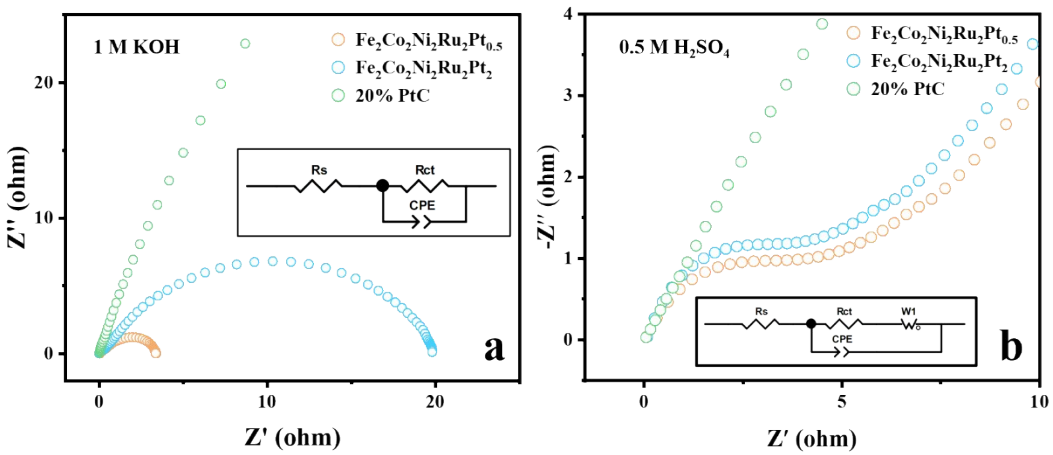

Fig. S9 (a) The Nyquist plots of $Fe_2Co_2Ni_2Ru_2Pt_{0.5}$, $Fe_2Co_2Ni_2Ru_2Pt_2$, and 20% Pt/C electrocatalyst in 1 M KOH solution. (b) The EIS Nyquist plots of $Fe_2Co_2Ni_2Ru_2Pt_{0.5}$, $Fe_2Co_2Ni_2Ru_2Pt_2$, and 20% Pt/C electrocatalyst in 0.5 M H_2SO_4 solution. Here R_s stands for electrolyte resistance, R_{ct} stands for charge transfer resistance, CPE stands for constant phase element and W1 stands for electrochemical reaction diffusion resistance.

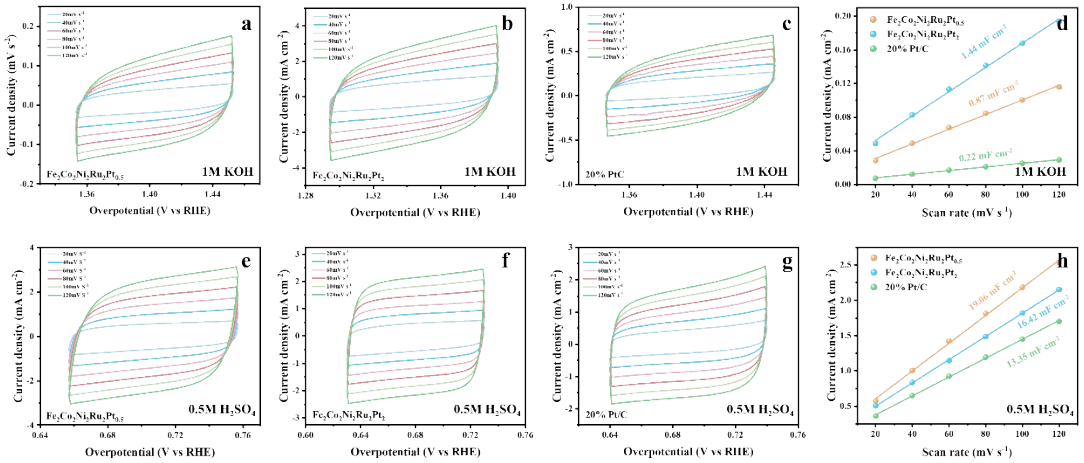

Fig. S10 ECSA evaluation for CV activation at different scan rates in 1 M KOH solution for (a) $Fe_2Co_2Ni_2Ru_2Pt_{0.5}$, (b) $Fe_2Co_2Ni_2Ru_2Pt_2$, (c) 20% Pt/C catalyst, and (d) corresponding C_{dl} values. ECSA evaluation for CV activation at different scan rates in 0.5 M H_2SO_4 solution for (e) $Fe_2Co_2Ni_2Ru_2Pt_{0.5}$, (f) $Fe_2Co_2Ni_2Ru_2Pt_2$, (g) 20% Pt/C catalyst, and (h) corresponding C_{dl} values.

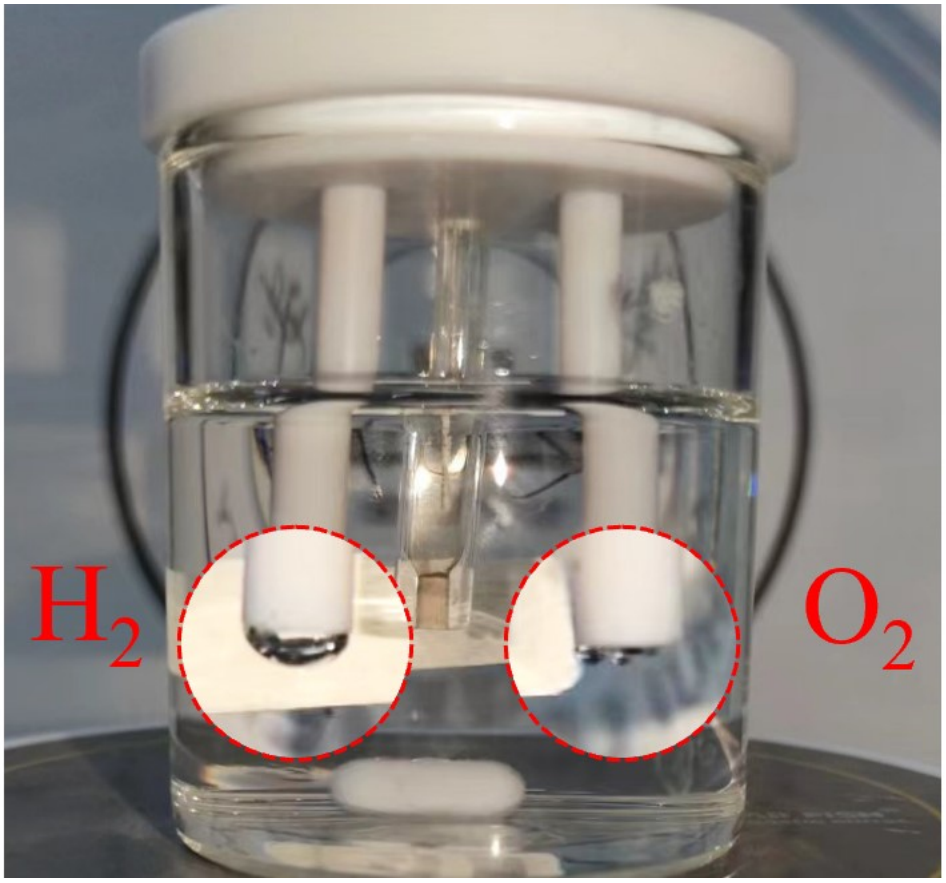

Fig. S11 Electrolysis experiment diagram of $Fe_2Co_2Ni_2Ru_2Pt_{0.5}$ in 1 M KOH solution.

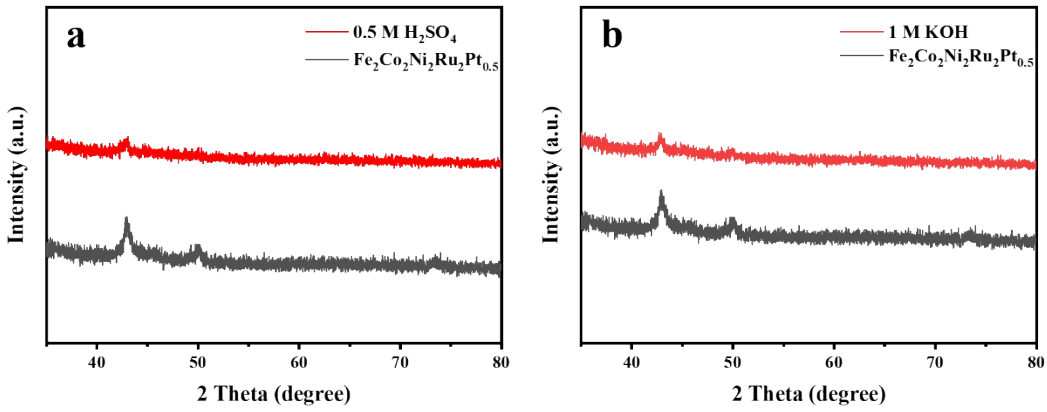

Fig. S12 XRD patterns of $Fe_2Co_2Ni_2Ru_2Pt_{0.5}$ before and after withstanding 30 hours of corrosion in different media: (a) after withstanding 30 hours of corrosion in 0.5 M H_2SO_4 solution, (b) after withstanding 30 hours of corrosion in 1M KOH solution.

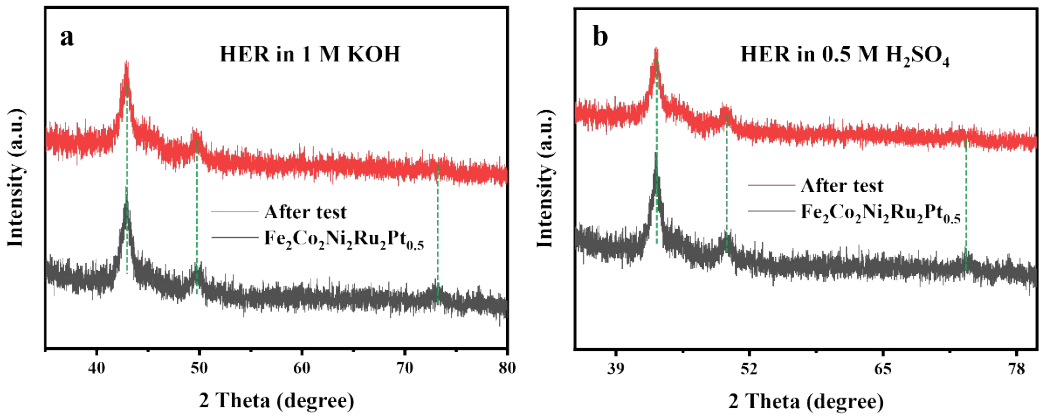

Fig. S13: XRD patterns before and after 12 h It test.

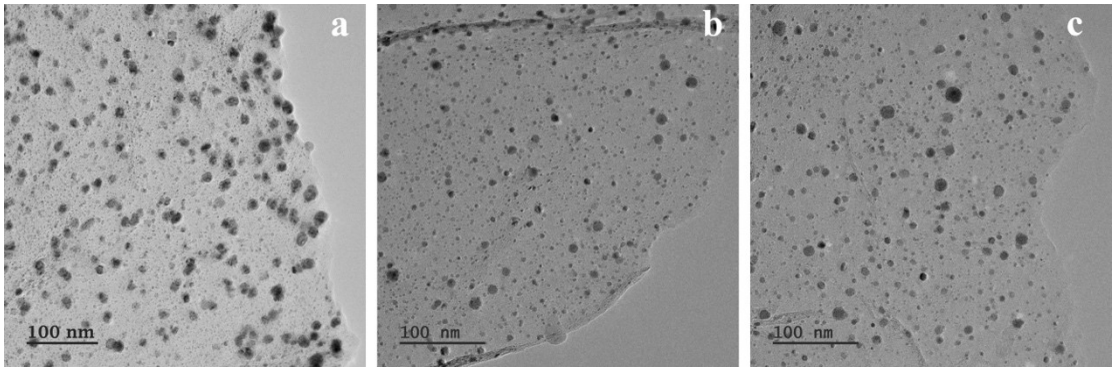

Fig. S14 TEM images of $Fe_2Co_2Ni_2Ru_2Pt_{0.5}$ after undergoing electrocatalytic reactions at other locations, (a) after undergoing electrocatalytic HER in 1 M KOH solution, (b) after undergoing electrocatalytic HER in 0.5 M H_2SO_4 solution and (c) after undergoing electrocatalytic OER in 1 M KOH solution.

Supplementary Tables

Table S1 EDS chemical composition (Atom%) analysis of $Fe_2Co_2Ni_2Ru_2Pt_{0.5}$.

Elemental content (Atom%)				
Fe	Co	Ni	Ru	Pt
19.7	18.5	15.6	35.6	10.6

Table S2 EDS chemical composition (Atom%) analysis of $Fe_2Co_2Ni_2Ru_2Pt_2$.

Elemental content (Atom%)				
Fe	Co	Ni	Ru	Pt
19.3	23.9	14.6	20.6	21.6

Table S3 The comparison of the electrocatalytic activities of $Fe_2Co_2Ni_2Ru_2Pt_{0.5}$ with some representative HER electrocatalysts recently reported in 1 M KOH.

Catalysts	η_{10} (mV)	Reference
PtNiCuMnLa HEA	62	1
PtPdCoNiMn HEA	48.7	2
FeCoNiCrMn HEA	69	3
FeCoNiPtRu HEA	104	4
FeCoNiCrMn HEA NPs	161.8	5
CC-S-HEA	115	6
RhRuPtPdIr HEA	65	7
FeCoNiCuTi HEA	64.9	8
CoNiFe (Cr/V) HEA	277	9
$FeCoNiCu_{0.5}$	71	10
PdPtRuRhAu HEA	70.7	11
PtNiCuMnMo HEA	44	12
This work	49.1	

η_{10}: Overpotential (mV) required to achieve a current density of 10 mA cm^{-2}.

Table S4 The comparison of the electrocatalytic activities of $Fe_2Co_2Ni_2Ru_2Pt_{0.5}$ with some representative HER electrocatalysts recently reported in 0.5 M H_2SO_4.

Catalysts	η_{10} (mV)	Reference
PtRuFeCoNi atomic layers	41.3	13
RhRuPtPdIr HEA	58	14
PtPdAuCuCo HEA	77	15
FeNiCuWRu HEA	49	16
AuPdFeNiCo HEA NPs	45	17
CoCrFeNiAl HEA	73	18
CoNiFe(Cr/V) HEA	45	9
$Pd_{0.2}Pt_{0.2}Ir_{0.2}Ru_{0.2}Rh_{0.2}$	42.2	19
NiCoFePtRh HEA	27	20
This work	40.8	

η_{10}: Overpotential (mV) required to achieve a current density of 10 mA cm^{-2}.

Table S5 The comparison of the electrocatalytic activities of $Fe_2Co_2Ni_2Ru_2Pt_{0.5}$ with some representative OER electrocatalysts recently reported in 1 M KOH solution.

Catalysts	η_{10} (mV)	Reference
NiMnFeCo	302	21
FeCoNiPtRu HEA	331	4
$FeCoNiCu_{0.5}$	377	10
Co-doped RuO_2 NWs	304	22
$Ni_{1.25}Ru_{0.75}P$	340	23
Ni_{50}(FeCoCrCu)	292.3	24
MoCoCu-P MEA	276.1	25
CoCuFeMoNiIrB	277	26
CuCoNiMnAl HEA	390	27
$Pt_{34}Fe_5Ni_{20}Cu_{31}Mo_9Ru$ HEA	259	28
HEA/PANI-CP	258	29
This work	275.6	

η_{10}: Overpotential (mV) required to achieve a current density of 10 mA cm^{-2}.

Table S6 EIS fitting results of $Fe_2Co_2Ni_2Ru_2Pt_{0.5}$, $Fe_2Co_2Ni_2Ru_2Pt_2$ and 20% Pt/C catalysts.

Reaction medium	Materials	R_s (Ω)	R_{ct} (Ω)
1 M KOH	$Fe_2Co_2Ni_2Ru_2Pt_{0.5}$	2.97	1.92
	$Fe_2Co_2Ni_2Ru_2Pt_2$	2.37	3.17
	20% Pt/C	2.16	11.91
0.5 M H_2SO_4	$Fe_2Co_2Ni_2Ru_2Pt_{0.5}$	9.16	5.25
	$Fe_2Co_2Ni_2Ru_2Pt_2$	9.17	5.43
	20% Pt/C	7.65	7.34

Table S7 EDS chemical composition (Atom%) analysis of $Fe_2Co_2Ni_2Ru_2Pt_{0.5}$ after HER in 1 M KOH solution.

Reaction medium	Elemental content (Atom%)				
1M KOH	Fe	Co	Ni	Ru	Pt
	13.4	15.7	20.2	39.3	11.4

Table S8 EDS chemical composition (Atom%) analysis of $Fe_2Co_2Ni_2Ru_2Pt_{0.5}$ after HER in 0.5 M H_2SO_4 solution.

Reaction medium	Elemental content (Atom%)				
0.5M H_2SO_4	Fe	Co	Ni	Ru	Pt
	2.6	2.5	2.6	12.6	79.7

Table S9 EDS chemical composition (Atom%) analysis of $Fe_2Co_2Ni_2Ru_2Pt_{0.5}$ after OER in 1 M KOH solution.

Reaction medium	Elemental content (Atom%)					
1M KOH-OER	Fe	Co	Ni	Ru	Pt	O
	7.5	10.0	8.8	16.9	2.0	54.8

References

1. T. Gu, F. Yu, Z. Yu, Y. Qi, Y. Li, F. Miao and Z. Yan, *J. Colloid Interface Sci.*, 2025, **688**, 308-316.
2. A. Chandran M, S. Sahoo, A. K. Singh and B. L. V. Prasad, *Small*, 2025, **21**, 2408317.
3. Y. Zhang, Q. Wan, L. Huang, T. Jiang, S. Wu, D. Li, Y. Liu, H. Wu and F. Ren, *J. Mater. Chem. A*, 2025, DOI: 10.1039/D5TA02103K.
4. M. Geng, Y. Zhu, J. Guan, R. Zhang, Q. Zou, L. Wang, B. Guo and M. Zhang, *J. Alloys Compd.*, 2024, **1005**, 176180.
5. X. Zhou, L. Zou, H. Zhu, M. Yan, J. Wang, S. Lan, S. Chen, H. Hahn and T. Feng, *Small*, 2024, **20**, 2310327.
6. Y. Liao, R. Zhu, W. Zhang, H. Zhu, Y. Sun, J. Chen, Z. Dong and R. Lv, *Nano Res.*, 2024, **17**, 3379-3389.
7. Y. Zou, L. Jing, J. Zhang, S. Luo, L. Wang, Y. Li, R. Goei, K. W. Tan and A. I. Yoong Tok, *J. Mater. Chem. A*, 2024, **12**, 5668-5678.
8. Y. He, J. Qin, F. Hu, L. Mao, B. Shen, T. M. Aminabhavi, Y. Vasseghian and A. Hojjati-Najafabadi, *Chem. Eng. J.*, 2024, **492**, 152145.
9. T. Nawaz, S. Ahmad, W. Abuzaid, F. Mustafa, W. Ahmad, S. El-Khatib, M. J. Kaddoura, A. H. Alami, H. Alawadhi and M. Egilmez, *APL Mater.*, 2025, **13**, 051114.
10. F. Guo, Y. Zhang, B. Shen, L. Wan, G. Hou, H. Cao, G. Zheng, Y. Zhao and H. Zhang, *J. Alloys Compd.*, 2024, **1002**, 175356.
11. Q. Wang, Y. Qin, J. Xie, Y. Kong, Q. Sun, Z. Wei and S. Zhao, *Adv. Mater.*, 2025, **37**, 2420173.
12. T. Gu, F. S. Yu, Z. Q. Yu, Y. X. Qi, Y. X. Li, F. Miao and Z. J. Yan, *J. Colloid Interface Sci.*, 2025, **688**, 308-316.
13. C.-Y. Wu, Y.-C. Hsiao, Y. Chen, K.-H. Lin, T.-J. Lee, C.-C. Chi, J.-T. Lin, L.-C. Hsu, H.-J. Tsai, J.-Q. Gao, C.-W. Chang, I. T. Kao, C.-Y. Wu, Y.-R. Lu, C.-W. Pao, S.-F. Hung, M.-Y. Lu, S. Zhou and T.-H. Yang, *Sci. Adv.*, **10**, eadl3693.
14. L. Jing, Y. Zou, R. Goei, L. Wang, J. A. Ong, A. Kurkin, Y. Li, K. W. Tan and A. I. Y. Tok, *Langmuir*, 2023, **39**, 3142-3150.
15. X. Chen, L. Su, Y. Tan, J. Yuan, Y. Mou, W.-Q. Deng and H. Wu, *J. Colloid Interface Sci.*, 2025, **691**, 137385.
16. Z. Lu, W. Sun, P. Cai, L. Fan, K. Chen, J. Gao, H. Zhang, J. Chen and Z. Wen, *Energy Environ. Sci.*, 2025, **18**, 2918-2930.
17. S. Jeong, A. J. Branco, S. W. Bollen, C. S. Sullivan and M. B. Ross, *Nanoscale*, 2024, **16**, 11530-11537.
18. P. Ma, M. Zhao, L. Zhang, H. Wang, J. Gu, Y. Sun, W. Ji and Z. Fu, *J. Materiomics*, 2020, **6**, 736-742.
19. C. Y. Lin, Z. Y. He, J. T. Lin, C. W. Chang, Y. C. Hsiao, S. C. Lin, Y. Chen, Y. M. Huang, S. C. Lee, C. W. Pao, K. H. Lin, A. J. Cowan and T. H. Yang, *Adv. Funct. Mater.*, 2025, DOI: 10.1002/adfm.202505927.
20. G. Feng, F. Ning, J. Song, H. Shang, K. Zhang, Z. Ding, P. Gao, W. Chu and D. Xia, *J. Am. Chem. Soc.*, 2021, **143**, 17117-17127.
21. X. Huo, Y. Zhang, H. Yu, S. Nie, X. Zuo, X. Xu and N. Zhang, *Int. J. Hydrogen Energy*, 2024, **87**, 505-514.
22. J. Wang, Y. Ji, R. Yin, Y. Li, Q. Shao and X. Huang, *J. Mater. Chem. A*, 2019, **7**, 6411-6416.

23. D. R. Liyanage, D. Li, Q. B. Cheek, H. Baydoun and S. L. Brock, *J. Mater. Chem. A*, 2017, **5**, 17609-17618.
24. Y. Pan, F. Zhao, G. Ji, S. Xu, R. Li, H. Zhou, R. Zhao, D. Zhao and F. Wu, *Int. J. Hydrogen Energy*, 2025, **127**, 147-159.
25. X. Wang, C. Yang, Y. Zhang, D. Xiong, S. Xu, L. Wang, L. Jiang, P. B. Sorokin and P. K. Chu, *J. Alloys Compd.*, 2024, **988**, 174332.
26. Z.-X. Cai, S. Bolar, Y. Ito and T. Fujita, *Nanoscale*, 2024, **16**, 4803-4810.
27. X. Zhu, J. Li, R. N. Ali and M. Song, *J. Power Sources*, 2024, **610**, 234738.
28. Z. Q. Chen, J. B. Wen, C. H. Wang and X. W. Kang, *Small*, 2022, **18**, 2204255.
29. L. Su, X. Chen, Y. Tan, W.-Q. Deng, H. Wu and X. Miao, *J. Mater. Chem. A*, 2025, **13**, 15743-15747.